



Shallow water table effects on water, sediment and pesticide transport in vegetative filter strips: Part A. non-uniform infiltration and soil water redistribution

Rafael Muñoz-Carpena¹, Claire Lauvernet², Nadia Carluer²

5 ¹University of Florida, Department of Agricultural and Biological Engineering, PO Box 110570, Gainesville, FL 32611-0570, USA

²Irstea, UR MALY, centre de Lyon-Villeurbanne, F-69626 Villeurbanne, France

Correspondence to: Rafael Muñoz-Carpena (carpena@ufl.edu)

Abstract. Vegetation buffers like vegetative filter strips (VFS) are often used to protect water bodies from surface runoff pollution from disturbed areas. Their typical placement in bottomland often results in the presence of a seasonal shallow water table (WT) that can decrease soil infiltration and increase surface pollutant transport during a rainfall/runoff event. Simple and robust components of hydrological models are needed to analyse the impacts of WT in the landscape. To simulate VFS infiltration under realistic rainfall conditions with WT, we propose a generic infiltration solution (Shallow Water table INfiltration algorithm: SWINGO) based on a combination of approaches by Salvucci and Entekhabi (1995) and Chu (1997) with new integral formulae to calculate singular times (time of ponding, shift time, and time to soil profile saturation). The algorithm was tested successfully on 5 distinct soils both against Richards's numerical solution and experimental data in terms of infiltration and soil moisture redistribution predictions, and applied to study the combined effects of varying WT depth, soil type, and rainfall intensity and duration. The results show the robustness of the algorithm and its ability to handle various soil hydraulic functions, and initial non-ponding conditions under unsteady rainfall. The effect of a WT on infiltration under ponded conditions was found effectively decoupled from surface infiltration/excess runoff processes for depths larger than 1.2 to 2 m, shallower for fine soils and shorter events. For non-ponded initial conditions, the influence of WT depth also varies with rainfall intensity. Also, we observed that soils with a marked air entry (bubbling pressure) exhibit a distinct behaviour with WT near the surface. The features and good performance of SWINGO support its coupling with an existing VFS model in the companion paper, where the potential effects of seasonal or permanent WTs on VFS pollutant transport and control are studied.

1 Introduction

The use of vegetative filter strips (VFS) can reduce sediment and surface runoff pollutants (i.e. sediment, colloids, nutrients, pesticides, pathogens) movement into receiving water bodies. The dense vegetation/soil system reduces runoff pollutants in three ways by increasing: a) soil infiltration that reduces total runoff volume (and dissolved runoff pollutants); b) surface



30 roughness that reduces surface velocity and produces settling of sediment and sediment-bonded pollutants; c) contact
between dissolved and particulate pollutants with the soil and vegetation surfaces that enhances their removal from runoff
(Muscutt et al., 1993; Muñoz-Carpena et al., 1999; Dosskey, 2001; Fox et al., 2010; Muñoz-Carpena et al., 2010; Yu et al.,
2013; Lambrechts et al., 2014; Wu et al., 2014). The efficiency of VFS in trapping pollutants is heavily influenced by the
highly variable spatial and temporal dynamics introduced by site-specific combinations of soil, climate, vegetation, and
35 human land use. For the case of runoff pesticides, these influences have been recognised in multiple field studies (Lacas et
al., 2005; Reichenberger et al., 2007; Poletika et al., 2009; Sabbagh et al., 2009). Other effects like hydraulic loading under
concentrated flow conditions (Fox et al., 2010) or timing of the pesticide application (Sabbagh et al., 2013) can also result in
reduced filter trapping efficiencies. As these systems are complex, the practice of using generic, simple regression equations
relating the reduction efficiency of pollutants with VFS physical characteristics (i.e. length, slope) is often inadequate (Fox
40 and Sabbagh, 2009).

Mechanistic understanding of VFS behaviour has advanced significantly in the last 20 years and numerical simulation tools
are available to analyse this important best management practice (BMP) under upland field conditions where runoff is
governed by excess rainfall and field inflow processes (Muñoz-Carpena et al., 1993, 1999; Abu-Zreig, 2001; Muñoz-
Carpena and Parsons, 2004; Poletika et al., 2009; Sabbagh et al., 2009; Carluer et al., 2017). A recent linked mechanistic
45 model has investigated multiple input factors and their relative importance and uncertainties of on the predicted reduction of
runoff, sediments, and pesticides (Fox et al., 2010; Lambrechts et al., 2014; Muñoz-Carpena et al., 2010, 2015).

However, because of their location near or at the riparian zone, VFS can at times be bounded by a seasonal shallow water
table (WT) (Borin et al., 2004; Ohlingerlow and Schulza, 2010). Examples of ubiquitous areas where these conditions exist
either seasonally or on a more permanent basis are humid coastal flatland zones, bottomlands near water bodies, and soils
with limiting horizons resulting in perched WTs. Generally, capillary effects from a WT can reduce infiltration and increase
50 subsequent runoff processes, and have a major effect on contaminant transport to surface waters (Gillham, 1984). In spite of
the potentially important environmental impacts of the presence of shallow water under VFS, there is a dearth of studies
addressing this problem either experimentally or mechanistically. Several authors suggest the importance of this factor in
VFS experimental studies (Lacas et al., 2005; Arora et al., 2010) or when designing or implementing this field BMP
55 (Simpkins et al., 2002; Dosskey et al., 2006, 2011), but they do not provide a mechanistic interpretation. Some authors
suggest that the reduction of infiltration and VFS efficiency can be problematic for seasonal WT depths above 2 m typical of
hydric soils (Dosskey et al., 2006, 2011; Lacas et al., 2012). As cited by Salvucci and Entekhabi (1995), the importance of
accounting for areas of WT effects in water balance and runoff studies has been recognized for a long time and specialized
analysis and simulation approaches have been proposed by numerous authors (for example, Vachaud et al., 1974; Srivastava
60 and Yeh, 1991; Salvucci and Entekhabi, 1995; Chu, 1997; Basha, 2000).

In spite of the ubiquity and importance of these areas and previous specialized analysis and modelling efforts, commonly
used field and watershed hydrological models are limited when describing infiltration and soil water redistribution with WT
(Beven, 1997, Liu et al., 2011). Among existing simulation approaches, solutions to the fundamental Richards (1931) partial



65 differential equation (RE) can describe the infiltration and redistribution of water in soil, including the specific case of when
a system contains a WT. However, RE does not have a general analytical solution and its application real-world systems
requires computationally intensive numerical approximations that can result in mass-balance and instability errors in some
cases (e.g. for coarse soils and highly dynamic boundary conditions) (Celia et al., 1990; Paniconi and Putti, 1994; Miller et
al., 1998; Vogel et al., 2001; Ross, 2003; Seibert et al., 2003). As a result, soil infiltration is often modelled in field and
watershed models using simpler physically-based approaches (Jury et al., 1991; Smith et al., 1993; Haan et al., 1994; Singh
70 and Woolhiser, 2002; Talbot and Ogden, 2008; Ogden et al., 2015). One of the most often used approaches in hydrologic
modelling is the Green-Ampt (1911) model adjusted to account for variable rainfall (Mein and Larson, 1973; Chu, 1978;
Skaggs and Khaleel, 1982). The model has the advantages of being computationally efficient and that its parameters can be
directly estimated from physical measurements, or derived indirectly from soil texture (Rawls et al., 1982, 1983). However,
the limitation of the original Green-Ampt model is that it assumes isotropic soil with uniform initial moisture content, and
75 saturated “piston” infiltration. Even with these non-realistic assumptions, if effectively parameterized, this method still
generates useful and reliable results compared with other numerical and approximated approaches (Skaggs et al., 1969; Mein
and Larson, 1973). Considering its advantages, Bouwer (1969) highlighted the utility of this method when taking into
account the computational trade-offs with RE solutions.

Extensions of the Green-Ampt model beyond its initial assumptions have enabled its application to other natural infiltration
80 cases, such as non-uniform soil profiles (Bouwer, 1969; Beven, 1984), and multistorm infiltration and redistribution (Ogden
and Saghafian, 1997; Smith et al. 2002; Gowdsh and Muñoz-Carpena, 2009). A particularly important case where an
extension of the original assumption of the Green-Ampt model is necessary is when there is a WT. In general, depth-
averaged soil moisture values in traditional infiltration equations like Green-Ampt (*i.e.* semi-infinite, uniform initial soil
moisture) overpredict infiltration estimations when the soil is bounded by a WT. This is due to the difficulty in obtaining an
equivalent initial uniform soil water content that effectively represents the real non-uniform water content condition with
85 WT (Salvucci and Entekhabi, 1995; Chu, 1997). Recently, Liu et al. (2011) presented a modification to Craig et al. (2010)’s
non-dimensional form of the Green-Ampt model to account for the presence of a WT. Although this modification is shown
to provide acceptable results as compared with a RE solution for a range of WT depths, the method assumes an initial
uniform soil water content profile, and its performance relies on an empirical correction between RE and standard Green-
90 Ampt results. Alternatively, previous works (Childs, 1960; Holmes and Colville, 1970; Duke, 1972) have suggested
describing the soil-water redistribution over a WT as an equilibrium hydrostatic condition (Fig. 1). This approach assumes a
linear relationship of soil matric potential (h , [L]) and soil depth (z , [L]) above the WT, whereby the non-uniform water
content of the soil (θ [L^3L^{-3}]) is described by the soil water characteristic curve, $\theta = \theta(h)$ (Jury et al., 1991),

$$h = L - z \Rightarrow \theta = \theta(L - z) \quad (1)$$

95 where L [L] is depth to the WT (*i.e.* the distance from the surface). Based on this initial and boundary hydrostatic
equilibrium conditions, Chu (1997) proposed an incremental calculation technique to evaluate infiltration into ponded soils
with a WT. This calculation relies on Bouwer (1969) expression of the Green-Ampt equation that accounts for infiltration of



water into a non-uniform soil as,

$$t = \int_0^{z_f} \left[\frac{\theta_s - \theta(L-z)}{f} \right] dz \quad (2)$$

100 where t [T] is time since the beginning of the event; θ_s [L^3L^{-3}] is the saturation water content; f [LT^{-1}] is the rate of surface infiltration; z_f [L] is the wetting front depth. Following Neuman, (1976), cumulative and instantaneous infiltration rate can be calculated by,

$$F_p = \int_0^{z_f} [\theta_s - \theta(L-z)] dz \quad (3)$$

$$f_p = K_s + \frac{1}{z} \int_0^{L-z_f} K(h) dh \quad (4)$$

105 where the subscript p denotes under ponding or "capacity", *i.e.* when the flux at the surface is not limited by available water and is therefore maximum for each time; K_s and $K(h)$ [LT^{-1}] represents the soil saturated hydraulic conductivity and unsaturated hydraulic conductivity function. Chu (1997) proposed the solution to eq. (2-4) using sufficiently small increments of z , $\Delta z = z_i - z_{i-1}$. If an initial value of F_i and f_i for the first Δz (from the surface to a small depth) is known, then successive values of time ($t_i = t_{i-1} + \Delta t$) for each Δz can be approximated by substituting eq. (3) into (2) as,

$$110 \quad t_i = t_{i-1} + dt = t_{i-1} + \frac{F_i - F_{i-1}}{0.5(f_i + f_{i-1})} \quad (5)$$

Chu (1997) further proposed that a valid initial step could be obtained by assuming standard Green-Ampt conditions (*i.e.* piston flow) from the surface, hydrostatic equilibrium of the surface water content with the WT (θ_o), and calculating the suction at the wetting front (S_{av}) as (Bouwer, 1964),

$$S_{av} = \frac{1}{K_s} \int_0^L K(h) dh \quad (6)$$

115 Vachaud et al., (1974) was able to use experimental data to test the solution of this equation successfully. However, their experimental data did not allow enough time to determine how the model would respond when the wetting front reaches L .

An elegant and useful approximate solution to ponded infiltration with WT was proposed by Salvucci and Entekhabi (1995). Their solution is based on the assumptions of initial hydrostatic equilibrium and uses Philip (1957) integral approximation of RE (Fig. 1). This approximate solution is advantageous, as it describes not only the infiltration but also soil water redistribution during infiltration, and the characteristics of the wetting front as it moves towards the WT during long events. 120 In addition, the method assumes a more realistic piecewise linear wetting front with a variable slope during infiltration (α in Fig. 1). This algorithm was successful when compared with RE solution for three different soil types and when tested with the soil moisture profile data from Vachaud and Thony (1971)'s experiments. However, the applicability of the algorithm for coupling with commonly used hydrological models is limited as it requires ponded conditions, Brooks and Corey's soil



125 water function (Appendix, eq. A1), and similarly to the original Green-Ampt it requires an implicit solution.
 The overall objective of this work and its companion paper is to analyse the impact of the presence of a WT on VFS
 efficiency. In this first paper, we will expand the Green-Ampt-based infiltration solution to soils bounded by WT under
 variable rainfall with no initial ponding. We accomplish this by combining Salvucci and Entekhabi (1995) and Chu (1997)
 approaches with a generic solution technique, and developing novel integral formulae to calculate the singular times (time to
 130 ponding, t_p , shift time t_0 , and time to column saturation, t_w) for soils with no initial ponding. We assess the ability of the
 simplified method to accurately predict surface infiltration and water content predictions for a variety of soils as compared
 with RE numerical solutions and previously published experimental data. An illustrative example of calculation during an
 unsteady rainfall event is also presented along with examples of applications of the proposed algorithm to analyse the effects
 of WT depth. In a companion paper, we couple the new shallow water infiltration algorithm with an existing VFS numerical
 135 model (VFSMOD) and analyse the effects on runoff, sediment and pesticide removal efficiency.

2 Proposed algorithm

2.1 Infiltration rate in soils bounded by a WT with a non-ponded initial state and subject to constant rainfall

In general, the infiltration rate (f [LT^{-1}]) of a WT bounded soil with uniform rainfall rate (i [LT^{-1}]) and no initial surface
 ponding will have a similar profile to the example shown in Fig. 2a, described by,

$$140 \quad \left\{ \begin{array}{ll} f = i & 0 < t \leq t_p \\ f = f_p & t_p < t < t_w \\ f = \min(f_w, i) & t \geq t_w \end{array} \right. \quad (7)$$

The identification of three singular times during the infiltration calculations is necessary for a solution to eq. (7). These three
 singular times are: a) time to reach ponding (t_p), b) shift time (t_0), and c) time to column saturation (t_w), when the wetting
 front approaches the capillary fringe at depth z_w (see Fig. 1). The effective saturation depth z_w relies on L and soil air entry
 pressure (h_b), $z_w = L - h_b$. Often, h_b is set at 0 (*i.e.* $z_w = L$), even if some of the soil characteristic functions take the air entry
 145 pressure into account (Brooks and Corey, 1964; Clapp and Hornberger, 1978). At t_w , the soil column is saturated and the rate
 of infiltration sharply drops to f_w , or i if $i < f_w$ (Fig. 2a). t_w depends on L and the slope of $K(h)$ (Salvucci and Entekhabi,
 1995). If the WT is very shallow, the time to saturation t_w can occur before the time to ponding. Salvucci and Entekhabi,
 (1995) and Liu et al., (2011) initially proposed that the infiltration rate is equal to $f_w = K_s$, when $t \geq t_w$, meaning that the
 vertical hydraulic gradient at the initial WT is 1. However, in most field situations when the wetting front has reached the
 150 WT, the profile's hydraulic gradient is less than 1 and the proposed solution might overestimate the final infiltration rate.
 Instead, another solution is to consider that for $t \geq t_w$ the infiltration flow at the surface (Q_f) is controlled by lateral drainage
 flow (Q_L) at the downslope boundary of the simulated soil elementary volume (Fig. 1b), applicable to bottomland conditions



typical of VFS. If we consider that the soil profile is saturated at $t \geq t_w$, and following Dupuit-Forchheimer assumptions (Van Hoorn and Van Der Molen, 1973) the discharge ($Q_f=Q_L$) can be estimated as,

$$155 \quad \left. \begin{aligned} Q_f &= f_w w b \\ Q_L &= K_{sh} S L w \end{aligned} \right\} Q_f = Q_L \Rightarrow f_w \approx \frac{K_{sh} S_o L}{b} \quad (8)$$

where K_{sh} is the lateral (horizontal) soil saturated hydraulic conductivity, w and b are the width and length of the VFS surface area, and S is the slope of the initial WT. In hillslope hydrological modelling S is typically assumed to equal soil surface slope (S_o) (Beven and Kirkby, 1979 ; Vertessy et al., 1993). If the position of the infiltration elementary volume is close to a draining stream where $S > S_o$, eq. (8) may underestimate the infiltration rate and a 2-dimensional drainage approach like
 160 Hooghoudt (1940) equation should be used instead (Kao et al., 2001; Ritzema, 1994; van Schilfgaarde, 1957). In the algorithm developed here, the two options for the boundary condition are implemented: with “lateral drainage” (eq. 8) and Vachaud’s “vertical drainage” ($f_w = K_s$).

2.2. Calculation of singular time points

Following Mein and Larson (1973), time to ponding t_p is the time for $f_p = i$ (intersection of the curves in Fig. 2a), typically
 165 when the surface water content is equal to saturation (Fig. 2c). At $t = t_p$ the equivalent wetting front depth (z_p) can be calculated by equating eq. (4) and (7),

$$f_p = K_s + \frac{1}{z} \int_0^{L-z} K(h) dh \quad \left| \begin{aligned} f &= i \\ \Rightarrow i &= K_s + \frac{1}{z_p} \int_0^{L-z_p} K(h) dh \Rightarrow z_p = \frac{1}{i - K_s} \int_0^{L-z_p} K(h) dh \end{aligned} \right. \quad (9)$$

Since equation (9) is implicit in z_p , it can be solved for each time step by defining the function $G_p: \mathbb{R} \rightarrow \mathbb{R}$, as well as its derivative dG_p/dz , so that the root $z_p \in [0, z_w]$ (*i.e.* $G_p(z_p) = 0$) is the wetting front depth at t_p ,

$$170 \quad \begin{aligned} G_p(z_p) &= z_p - \frac{1}{i - K_s} \int_0^{L-z_p} K(h) dh \\ \frac{dG_p(z_p)}{dz} &= 1 + \frac{K_s}{i - K_s} \frac{K(L - z_p)}{K_s} \end{aligned} \quad (10)$$

z_p can be obtained applying a bracketed Newton-Raphson algorithm (Press et al., 1992). Here, we denote k as the Newton-Raphson iteration level, thereby obtaining,

$$z_p^{k+1} = z_p^k - \frac{G_p(z_p^k)}{\frac{dG_p(z_p^k)}{dz}} \quad \text{with} \quad |z_p^{k+1} - z_p^k| < \varepsilon \quad (11)$$



with ε as the error tolerance (here, it is set to 10^{-8}). From eq. (3) at $t=t_p$ ($z=z_p$) and $F_p=i \cdot t_p$ we obtain,

$$175 \quad t_p = \frac{1}{i} \left(\theta_s z_p + \int_L^{L-z_p} \theta(h) dh \right) \quad (12)$$

Next to ensure that F_p and $i \cdot t_p$ match at the intersection of the two curves (Fig. 2b), an abscissa translation (shift time, t_0) is applied to F_p (Mein and Larson, 1973). Setting $z=z_p$ on eq. (2) yields t_0 as,

$$t_0 = \int_0^{z_p} \left[\frac{\theta_s - \theta(L-z)}{f(z)} \right] dz \quad (13)$$

Lastly, t_w is determined by calculating the integral eq. (2) at $z_F=z_w=L-h_b$ (Fig. 1) and adjusting for t_p and t_0 ,

$$180 \quad t_w = t_p - t_0 + \int_0^{z_w} \frac{\theta_s - \theta(L-z)}{f(z)} dz \quad (14)$$

and using eq. (3), the cumulative infiltration at t_w is determined by,

$$F_w = \theta_s z_w - \int_{h_b}^L \theta(h) dh \quad (15)$$

t_w is equivalent to the non-dimensional time X_c proposed by Liu et al., (2011) that relies on the empirical error correction between RE solution and the Green-Ampt model. However, here t_w (eq. (14)) is calculated analytically for the more general case of non-uniform soil water content.

2.3 Infiltration capacity algorithm after surface ponding

The solution of Salvucci and Entekhabi (1995)'s can be simplified by setting the wetting front slope to zero (*i.e.* a horizontal front ($\alpha=0$) at the depth z_F , Fig.1). This approach reduces the solution, making it analogous to eq. (2), which was employed by Bouwer (1969) in his explanation of the Green-Ampt model's applicability. For initial non-ponding conditions, the equation becomes,

$$190 \quad t = t_p - t_0 + \int_0^{z_F} \frac{\theta_s - \theta(L-z)}{K_s + \frac{1}{z} \int_0^{L-z} K(h) dh} dz \quad ; t_p < t < t_w \quad (16)$$

As the wetting front travels deeper into the soil, α could increase, contingent on the type of soil (e.g. α is larger for fine soils). However, as the wetting front approaches WT, the pore space available for infiltration is small, which limits the error of the calculations (Salvucci and Entekhabi, 1995). This assumption is tested in section 2.4.

195 To solve for $z=z(t)$ using the z -implicit eq. (16), we specify the function G : as $\mathbb{R} \times \mathbb{R}^+ \rightarrow \mathbb{R}$ and its derivative as dG/dz , so that the root $z \in [z_{i-1}, z_w]$ of the function G is equal to the depth of the wetting front for a given time t ,



$$G(z, t) = t - t_p + t_0 - \int_0^z \frac{\theta_s - \theta(L-z)}{K_s + \frac{1}{z} \int_0^{L-z} K(h) dh} dz$$

$$\frac{dG(z, t)}{dz} = - \frac{\theta_s - \theta(L-z)}{K_s + \frac{1}{z} \int_0^{L-z} K(h) dh}$$

$$z^{k+1} = z^k - \frac{G(z^k, t)}{\frac{dG(z^k, t)}{dz}} \quad \text{with} \quad |z^{k+1} - z^k| < \varepsilon \quad (17)$$

In summary, for each time increment the proposed algorithm computes the depth of the wetting front, $z_{Fi}=z_i$ (eq. 17), F (eq. 3, 15) and f (eq. 7-8 and 4) using the singular times auxiliary eq. (12-14). A bracketing step in the Newton-Raphson algorithm is necessary, as the function G is undefined outside its physical range ($z_p < z < z_w$). The proposed algorithm is generic in that it can be used with any soil hydraulic functions like those of Gardner (1958), van Genuchten (1980) or Brooks and Corey (1964) (Appendix A) if numerical integration is used. Here, we used a Gauss-Quadrature integration scheme (Abramowitz and Stegun, 1972; Press et al., 1992).

2.4 Infiltration of soils with a WT and variable rainfall without initial ponding

For real VFS field situations, unsteady rainfall without initial soil ponding must be considered. The runoff produced by excess infiltration (*i.e.* Hortonian) and WT saturation (*i.e.* Dunne) are then determined at each time by water balance at the surface without accounting for evaporation during the rain event (Chu, 1997),

$$\Delta P = \Delta F + \Delta S + \Delta RO \quad (18)$$

where Δ is the increment for that rainfall period, P and RO [L] are cumulative precipitation and excess rainfall (runoff volume), respectively, and s is the surface storage ($0 < s < s_{max}$). When present, the surface storage term (*i.e.* non-zero s_{max}) acts as a reservoir that must be filled ($s=s_{max}$) before runoff is generated (Chu 1978; Skaggs and Khaleel, 1982). Non-uniform rainfall is described by a hyetograph as a series of constant rainfall periods j (*i.e.* $i=i_j$ for $t_j < t < t_{j+1}$). After the initial rainfall period (*i.e.* t_j with $j>1$) and when surface storage becomes zero, t_p (and t_0) must be recomputed for the subsequent rainfall event (Chu, 1978),

$$t_p = \frac{1}{i_j} \left[\left(\theta_s z_p + \int_L^{L-z_p} \theta(h) dh \right) - P(t_j) + RO(t_j) \right] + t_j \quad (19)$$

Also, each time t_p , and t_0 are calculated, t_w has to be re-calculated. $t_p = t_0 = 0$, at the beginning of the event when ponding is present.

To allow for predictions of soil water content redistribution during the event (Fig. 1) and to maintain mass balance during infiltration for alternating periods of ponding and non-ponding conditions, it is necessary to track the “effective” position of the wetting front z_F for periods with no ponding. To do this, the value of z_F must satisfy the total cumulative infiltration amount at every time step, F_z (Fig. 1) such that,

$$F_z = \theta_s z_F + \int_L^{L-z_F} \theta(h) dh = \theta_s z_F - \int_0^{z_F} \theta(L-z) dz \quad (20)$$

which is an implicit equation in z_F and as before requires finding the root $z_F \in [z_{F_{i-1}}, z_w]$ ($z_{F_{i-1}}$ is the wetting front depth at previous time step) of the function $G_F: \mathbb{R} \rightarrow \mathbb{R}$ such as:

$$225 \quad \left. \begin{aligned} G_F(z_F) &= F_z - \theta_s z_F - \int_L^{L-z_F} \theta(h) dh \\ \frac{dG_F(z_F)}{dz} &= -\theta_s + \theta(L-z_F) \end{aligned} \right| \Rightarrow \begin{aligned} z_F^{k+1} &= z_F^k - \frac{G_F(z_F^k)}{\frac{dG_F(z_F^k)}{dz}} \\ |z_F^{k+1} - z_F^k| &< \varepsilon \end{aligned} \quad (21)$$

The wetting front depth estimates play a key role in hydrological applications where the aim is to simulate the potential for direct contamination of the WT by pollutants.

The next section provides an illustrative application of the full algorithm (herein referred as SWINGO: Shallow Water table Infiltration aLgorithm) under unsteady rainfall conditions, typical in VFS settings (see Supp. Materials for coding details, source code, inputs and outputs).

3 Testing and applications

3.1 Numerical testing

A first step to validate SWINGO is done for the case of initially ponded soil and steady rainfall by a comparison with a finite difference mass-conservative numerical solution of RE (Celia et al., 1990) using Nofziger and Wu, (2003)'s CHEMFLO-2000 model. We used four soils that represented a variety of attributes. The Brooks and Corey soil water attributes and hydraulic conductivity curves (Table 1) were used for the initial soil description, and this description was later compared with van Genuchten parameters yielding similar results (results not shown). The first 3 soils represent typical clay, silty loam, and sandy loam soils with a 1.50 m deep WT (Salvucci and Entekhabi, 1995). The fourth soil corresponds to a fine sandy soil experimentally studied by Vachaud and Thony (1971) with a WT at 1.01m.

The soil water initial condition in CHEMFLO-2000 was set to hydrostatic equilibrium with a WT (eq. 1). The bottom boundary condition was set to a fixed matric potential $h(z=L) = 0$, to be representative of a WT at depth L . To simulate rainfall, the top boundary condition is set to a mixed type boundary with the flux density equal to the specified rainfall rate and the critical matric potential equalling zero (Nofziger and Wu, 2003). To allow for the development of distinct t_p and t_w values during the simulation, the constant rates of rainfall were chosen based on the soil texture. This selection was done utilizing a ratio of $i/K_s=6$ for the fine soils (clay and silty loam) and $i/K_s=2$ for the coarse soils, corresponding to the sandy loam and fine sandy soils studied by Vachaud and Thony (1971).

The comparison of the relative infiltration rates (f/K_s) calculated by RE (symbols) and the proposed SWINGO (lines) for the



case of vertical drainage end boundary condition ($f_w = K_s$) is shown in Figure 3. The performance of the algorithm is similar to RE for all soils studied. The median efficiency coefficients C_{eff} (Nash and Sutcliffe, 1970) ranged from 0.927–0.9997, with the highest values being for clay, and yielding statistically acceptable models at 0.01 level of significance (Ritter and Muñoz-Carpena, 2013) (Table 1). For the same clay soil with ponded conditions and a WT, Salvucci and Entekhabi (1995) reported errors of approximately 5% at time t_w , at the point when the wetting front reaches the WT saturation (z_w), and the infiltration rate switches to the saturated hydraulic conductivity $f_w = K_s$ ($f/K_s = 1$). Smaller differences (1% for clay and sandy loam and 3% for the rest) were found between both solutions in our tests. These observations indicate that the simplification (horizontal wetting front, $\alpha=0$) did not affect the predicative ability of the rate infiltration. A crucial pattern to notice is that the estimates of time to ponding acquired across our tested soil types and normalized rates of rainfall closely matched the outputs of the RE solution. Our results also indicate that the use of the non-uniform integral equations (eq 9-12) effectively limit errors in the t_p estimation that sometimes occur when utilizing the Green-Ampt model (Barry et al., 1996).

Figure 4 displays the cumulative infiltration and the depth of the wetting front determined using eq (20-21) for the vertical drainage boundary condition for the cases from Table 1. Similar to the infiltration curves, z_F values exhibited a plateau at t_w as they reach column saturation (Fig. 4b), corresponding to the capillary fringe at a depth of $z_F = z_w = L - h_b$ (Fig. 1), and therefore are not equal to the depth of the WT (fine sand: $L=1.01$ m; other soil types: $L=1.50$ m).

As the simplified approach is able to produce reliable z_F predictions, it also allows for the depiction of the redistribution of the soil water content during infiltration. We display the predictions of soil water (Figure 5) calculated by the proposed algorithm (dashed lines) as compared with the outputs of the RE solution (solid lines) for the non-ponding numerical test examples used previously. The simplified model is able to identify the midpoint of the wetting front depth at all time points. Additionally, our simplification of including the horizontal wetting front ($\alpha=0$) generates an accurate prediction of soil water at earlier time points for all soil types, but this prediction decays somewhat at later time points when approaching column saturation for fine soils. The model does not degrade at later time points for the sandy soil type when it matches a horizontal wetting front redistribution. As mentioned previously, because of the smaller pore space near column saturation, the mass errors generated by non-zero slopes stay negligible. The infiltration mass balance error at the end of the simulation (Fig. 4a) ranges from 3–8%. This range of error values is deemed satisfactory, as these errors are the summation of approximation errors of both the infiltration and redistribution of soil moisture generated during the simulation.

3.2 Experimental testing

The physics of the model were tested in a second step using experimental data from Vachaud et al., (1974) and Chu, (1997). The data collected in the laboratory represents infiltration under ponded conditions in a vertical column of fine sand soil with a WT at 0.925 m depth. To demonstrate the generality of the proposed algorithm, the Vachaud et al., (1974) measured soil hydraulic characteristics were fitted to van Genuchten soil water characteristic and related unsaturated hydraulic conductivity function based on Mualem (1976) simplification (vG/vG), and the later was also fitted to Gardner function (vG/Grd) (see Appendix A and soil parameters in Table 1). The goodness-of-fit of these hydraulic functions (inset of Fig. 6) shows a small



improvement of the $K(h)$ function for Gardner over that of van Genuchten-Mualem against the experimental data.

The simulated relative infiltration rates obtained with the proposed algorithm matched the observed data well ($C_{\text{eff}}=0.913-0.942$, RMSE for $f=5.07 \times 10^{-6}-6.20 \times 10^{-6}$ m/s), yielding statistically acceptable models at $\alpha=1\%$ for vG/Grd and $\alpha=5\%$ for vG/vG combinations (Ritter and Muñoz-Carpena, 2013) (Table 1). The main differences observed between approximated solutions with vG/Grd or vG/Grd soil water functions are near the time when the wetting front depth approaches the WT, with a small advance (~ 0.1 h) introduced by the vG/Grd option. These small differences are related to the slope of the wetting front being different than 0, especially close to the intersection with the WT at the end of the event (Fig. 5). Note also that in this experimental case no observed data was available for comparison at the time when the wetting front reached the WT.

In all, these results provide not only a test of the simplified model against experimental data, but also illustrate its robustness and flexibility to handle other soil hydraulic functions.

3.3 Illustration for unsteady rainfall conditions

The use of SWINGO to simulate realistic unsteady rainfall conditions is presented for a storm composed of 4 rainfall periods: $i_1=1$ cm/h ($0 < t \leq 2.8$ h), $i_2=0.25$ cm/h ($2.8 < t \leq 4.2$ h), $i_3=1$ cm/h ($4.2 < t \leq 5$ h) and $i_4=0.25$ cm ($5 < t \leq 6.9$ h) (Table 2 and Fig. 7). The soil is clay (Table 1) with bottom vertical drainage boundary condition and $s_{\text{max}}=0$ (*i.e.* no surface storage). At the beginning of the event the soil is not ponded and is in equilibrium with the WT at 150 cm below the surface. For the initial period, we calculate first the time to ponding with eq. (9-12, 19) ($t_p=4657.2$ s= 1.29 h), the corresponding t_0 (2319 s= 0.64 h) with eq. (13), and the time to reach the WT t_w (16100 s= 4.47 h) with eq. (14). Since the t_w is higher than the rainfall period and t_p lower than the rainfall period, infiltration is equal to the rainfall rate ($f=i_1$; $0 < t < t_{p1}$) before ponding. After ponding it follows the infiltration capacity curve described by the solution of eq (16-17). At the beginning of the second rain period, since the new rainfall rate is less than the infiltration rate at the end of the previous period ($i_2=0.25$ cm/h $< f_p=0.52$ cm/h) and t_w is still beyond the period, the infiltration rate equals the new rainfall rate ($f=i_2$). At the beginning of the third period, the new rainfall rate is larger than the corresponding potential infiltration rate at that time ($i_3=1$ cm/h $> f_p=0.44$ cm/h) and ponding starts again immediately such that the new $t_p=t_3$ (15000 s= 4.2 h, beginning of the new rainfall period), and t_0 (13764 s= 3.82 h) and t_w (18500 s= 5.14 h) are recalculated. Since t_w is beyond the period, the infiltration is maintained at capacity for the duration of this rainfall period. For the last period, the rainfall rate is lower than the ending infiltration capacity for last period ($i_4=0.25$ cm/h $< f_p=0.34$ cm/h), and infiltration is initially set to the rainfall rate. However, since t_w is within this period, the soil saturates when the water front reaches the WT depth ($t \geq t_w$), and this results in saturated vertical drainage flow with unit hydraulic gradient $f=f_w=K_s$ (eq. 7-8) until the end of the storm. The values of the wetting front position (z_f) in Table 2 are calculated from the solution of eq (17) during infiltration capacity (ponding) periods, and the equivalent depths described by eq. (21) during non-ponding periods. Similarly, cumulative totals are calculated with eq. (3) or (20), and excess rainfall amounts are calculated with the surface mass balance eq. (18) for every time step.



3.4 Evaluation of WT effects on infiltration under conditions of ponding and non-ponding

315 Figure 8 presents the effect of the WT depth variation ($L=0-200$ cm) and event duration ($0.5 < D < 6.0$ h) on cumulative infiltration under ponding conditions for the soils in Table 1. The two end time boundary conditions are compared: f_w vertical (a-d) and f_w lateral (e-h). For the conditions tested it is possible to identify three clearly defined regions (denoted I, II and III in Fig. 8) based on the influence of the WT depth on the cumulative infiltration. Region I (left, shaded in Fig. 8) represents the WT near the surface, *i.e.* when it is within the capillary fringe area $L < h_b$ (Fig. 1). The position of the WT in this region does not affect infiltration since the soil column is already saturated regardless of L with $F=D \cdot f_w$. Next, Region II (clear background on Fig. 8a-d) is the most sensitive to variations of WT depth, located between $L=h_b$ and a limit depth ($L=125-180$ cm) where the variation of F is small (slope less than 0.2%). This limit depends on the shape of the soil water characteristic curve for each soil. Finally, Region III represents a region where surface infiltration can be considered effectively decoupled from the presence of the WT.

325 Next, the robustness and physical behaviour of the algorithm under non-ponded initial conditions was tested with different rainfall rates ($i=0.1-20$ cm/h), event durations ($D=1-12$ h) and WT depths ($L=0-400$ cm). Fig. 9a-d summarizes the results for $D=6$ hours and the vertical drainage boundary condition ($f_w = K_s$). Two main effects are identified. Firstly, as expected F is insensitive to changes in L for rainfall intensities lower than K_s , when $f=i$ (no ponding) and $F=D \cdot K_s$. Notice that this effect, although present, is not visible in the clay soil (Fig. 9b) since the K_s is below the first contour line. Secondly, for rainfall rates above K_s , the sensitivity to L varies by soil, depending on h_b and the time to ponding values for each rainfall rate (eq. 12). As in the ponding case, the soil column is saturated when $L \leq h_b$, and there is no sensitivity below this depth. In finer, less permeable soils (Fig. 9a-b) ponding happens earlier for the same rainfall rate i , resulting in an increased sensitivity to L with lower rainfall rates. For the lateral drainage boundary condition, results are similar for the finer soils (Fig. 9e-f), but much more sensitive to WT depth and rainfall rate values for more permeable soils (Fig. 9g-h).

335 Importantly, since excess rainfall runoff (RO) is complementary to F (eq. 18), these results also quantify the important influence that the combined effects of WT, soil type and rainfall intensity can have on surface runoff flow and transport processes in the VFS.

Summary and Conclusions

340 Limitations in current modelling approaches hamper the evaluation of the effects of WTs on soil infiltration and runoff in vegetative filter strips (VFS). A promising way to overcome these issues is by utilizing simplified yet realistic specialized algorithms in conjunction with available hydrological models to evaluate the impact of WTs in the environment. Previously, Salvucci and Entekhabi, (1995) and Chu, (1997) recommended the use of Green-Ampt implicit integral equations to examine infiltration into ponded soils with WT. We developed and assessed a simplified generic algorithm that is appropriate for coupling with available hydrological models, in particular the study of WT effects on VFS runoff pollution control performance. The proposed SWINGO algorithm is generic— it can utilize any configuration of soil hydraulic functions—

345



and can be operated under non-ponded, ponded, and realistic variable rainfall conditions to determine runoff (excess rainfall), infiltration, and soil-water redistribution during the event.

350 SWINGO performed well (C_{eff} from 0.91 to 0.99) in comparison with the RE solution and using experimental data on 5 representative soils. The algorithm also was able to describe successfully the soil water redistribution during the simulated event. These useful and reliable predictions indicate that the proposed approach incorporating a horizontal slope of the wetting front is suitable for most real-world applications. Through an application of our proposed SWINGO algorithm, we showed the sensitivity of the infiltration and excess runoff to the depth of the WT, the length and intensity of the rainfall event, the soil texture and drainage bottom condition.

355 Some of the limitations of the proposed algorithm are the assumptions of a homogeneous soil profile and horizontal wetting front for fine soils. Future research is recommended to determine the general validity of the assumption of a hydrostatic equilibrium and the proposed computation of singular points during the infiltration episode. Additional experimental testing of the model should be conducted using data collected under various experimental and natural conditions (especially during events long enough for the wetting front to reach the WT).

360 As SWINGO was accurate, fast, and robust when analysing a variety of conditions, it is appropriate to couple with currently available hydrological models to gauge the influence of the presence of WTs on other processes on the landscape. The dynamic coupling with overland flow and transport processes in the VFS is developed in the companion paper. Global sensitivity and uncertainty analysis of the coupled model is conducted to identify important input factors and their interactions that will provide better understanding of the fundamental processes controlling VFS efficiency under WT conditions, and guide users to select effective parameters for practical applications.

365 Appendix A

The Brooks and Corey (1964) soil water characteristic ($\theta=\theta(h)$) and hydraulic conductivity ($K=K(h)$) functions are defined as,

$$S_e = \frac{\theta - \theta_r}{\theta_s - \theta_r} = \begin{cases} (h/h_b)^{-\lambda} & ; h > h_b \\ 1 & ; h_b \geq h \end{cases} \quad (A1)$$

$$K(h) = K_s S_e^\eta$$

370 with h_b = bubbling pressure [L, < 0] ; λ = Brooks and Corey pore size index (shape parameter); η = Brooks & Corey hydraulic conductivity shape parameter, often $\eta = 3+2/\lambda$. θ_s and θ_r are the saturated and residual water content [L³L⁻³].

The van Genuchten (1980) soil water characteristic and hydraulic conductivity curves are defined as,



$$S_e = \frac{\theta - \theta_r}{\theta_s - \theta_r} = \begin{cases} (1 + (\alpha_{vG} h)^n)^{-m} & ; h > 0 \\ 1 & ; h \leq 0 \end{cases} \quad (A2)$$

$$K(h) = K_s S_e^{1/2} \left(1 - (1 - S_e^{1/m})^m \right)^2$$

where $\alpha_{vG} [L^{-1}] > 0$, n, m are shape parameters. The Gardner (1958) unsaturated hydraulic conductivity function is given by,

$$K(h) = \begin{cases} \frac{K_s}{1 + (h/h_c)^{n_{Grd}}} = \frac{K_s}{1 + (\alpha_{Grd} h)^{n_{Grd}}} & ; h > 0 \\ K_s & ; h \leq 0 \end{cases} \quad (A3)$$

375 where $h_c = 1/\alpha_{Grd}$ = matric potential constant ($5 < h_c < 50$), and n_{Grd} = empirical constant ($1.8 < n_{Grd} < 3.5$).

Nomenclature

h	[L]	soil matric potential	h_b	[L]	capillary suction (bubbling pressure)
$\theta = \theta(h)$	$[L^3 L^{-3}]$	soil water characteristic	θ_s	$[L^3 L^{-3}]$	saturated water content
$K = K(h)$	$[LT^{-1}]$	hydraulic conductivity	K_s	$[LT^{-1}]$	saturated hydraulic conductivity
F	[L]	cumulative infiltration	F_p	[L]	cumulative infiltration at t_p
f	$[LT^{-1}]$	actual infiltration at surface	f_p	$[LT^{-1}]$	infiltration capacity (ponding)
i	$[LT^{-1}]$	rainfall rate	L	[L]	water table depth
S_{av}	[L]	suction at the wetting front	z_F	[L]	depth of the wetting front
t_w	[T]	time to column saturation	z_w	[L]	effective depth of saturation
t_p	[T]	time to ponding	z_p	[L]	wetting front depth at t_p
t_0	[T]	shift ponding time	RO	[L]	cumulative excess rainfall
P	[L]	cumulative precipitation	s	[L]	surface storage
D	[T]	storm duration			

Author contribution

RMC and CL developed conceptual model, code and testing. NC contributed to the theoretical development. RMC and CL
 380 prepared the manuscript with contributions from all co-authors.



Acknowledgements

We thank G. Salvucci for providing valuable insight and relevant information from his original efforts on this topic, J.V. Giráldez for providing useful and important references for this project, and J. Vanderborcht for his invaluable comments on the lateral drainage boundary condition development. We also thank the ECPA, DGPAAT and IRSTEA for financial support during RMC's sabbatical in France that made this research possible. RMC also acknowledges the UF Research Foundation Professorship, UF Water Institute Fellowship, and USDA NIFA Award No. 2016-67019-26855 that provided additional support.

References

Abramowitz M., Stegun I.A.: Handbook of Mathematical Functions with Formulas, Graphs, and Mathematical Tables. National Bureau of Standards Applied Mathematics Series 55. 10th Printing, 1972.

Abu-Zreig, M.: Factors affecting sediment trapping in vegetated filter strips: simulation study using VFSMOD. Hydrological Processes 15, 1477–1488. doi:10.1002/hyp.220, 2001.

Arora, K., Mickelson, S.K., Helmers, M.J., Baker, J.L.: Review of Pesticide Retention Processes Occurring in Buffer Strips Receiving Agricultural Runoff. JAWRA Journal of the American Water Resources Association 46, 618–647, doi:10.1111/j.1752-1688.2010.00438.x, 2010.

Barry, D. A., Parlange, J.-Y., Haverkamp, R.: Comment on “Variable-Head Ponded Infiltration Under Constant or Variable Rainfall” by J. R. Philip, Water Resour. Res., 32(5), 1467–1469, doi:10.1029/95WR03645, 1996.

Basha HA.: Multidimensional linearized nonsteady infiltration toward a shallow water table. Water Resour. Res., 36(9):2567-2573, doi:200010.1029/2000WR900150, 2000.

Beven K., J., Kirkby M.J.: A physically based variable contributing area model of basin hydrology. Hydrological Sciences Bulletin, 24:43-69, doi: 10.1080/02626667909491834, 1979.

Beven K.: Infiltration into a class of vertically non-uniform soils. Hydrological Sciences Journal, 29(4), 425, doi:10.1080/02626667909491834, 1984.

Beven, K. TOPMODEL: A critique. Hydrol. Proc., 11, 1069-1085, 1997.

Bouwer H.: Infiltration of water into nonuniform soil. J. Irrigat. Drain. Div., 95(IR4):451–462, 1969.

Bouwer H.: Unsaturated flow in ground-water hydraulics. Hydraul. Div. Amer. Soc. Civil Eng., 90(HY5), 121-144, 1964.

Brooks, RH, Corey AT.: Hydraulic properties of porous media. Hydrol. Paper., 3, 1964.

Carluer, N., Lauvernet, C., Noll, D., Muñoz-Carpena, R.: Defining context-specific scenarios to design vegetated buffer zones that limit pesticide transfer via surface runoff, Sci. Total Environ., 575, 701-712, doi:10.1016/j.scitotenv.2016.09.105, 2017.

Celia M.A., Bouloutas E.T., Zarba RL.: A general mass-conservative numerical solution for the unsaturated flow equation. Water Resour. Res., 26(7):1483-1496, 1990.



- Childs E.C.: The nonsteady state of the water table in drained land. *J. Geophys. Res.*, 65(2), 780-782, 1960.
- Chu ST.: Infiltration during an unsteady rain. *Water Resour. Res.*, 14(3), 461-466, 1978.
- 415 Chu ST.: Infiltration model for soil profiles with a water table. *Trans. ASAE.*, 40(4), 1041-1046, 1997.
- Clapp, R. B., and G. M. Hornberger: Empirical equations for some soil hydraulic properties, *Water Resour. Res.*, 14(4), PP. 601-604, 1978.
- Craig JR, Liu G, Soulis ED.: Runoff–infiltration partitioning using an upscaled Green–Ampt solution. *Hydrol. Process.* 24, 2328-2334, doi:10.1002/hyp.7601, 2010.
- 420 Dosskey, M.G., Helmers, M.J., Eisenhauer, D.E.: A design aid for sizing filter strips using buffer area ratio. *Journal of Soil and Water Conservation* 66, 29–39. doi:10.2489/jswc.66.1.29, 2011.
- Dosskey, M.G., Helmers, M.J., Eisenhauer, D.E.: An Approach for Using Soil Surveys to Guide the Placement of Water Quality Buffers. *Journal of Soil and Water Conservation* 61, 344–354, 2006.
- Dosskey, M.G.: Toward quantifying water pollution abatement in response to installing buffers on crop land. *Environ Manage* 28, 577–598, doi: 10.1007/s002670010245, 2001.
- 425 Duke HR. Capillary properties of soils - influence upon specific yield. *Trans. ASAE.* 15(4):688-691, 1972.
- Fox, G., Muñoz-Carpena, R., Sabbagh, G.: Influence of flow concentration on parameter importance and prediction uncertainty of pesticide trapping by vegetative filter strips. *J. Hydrol.*, 384, 164-173, doi:10.1016/j.jhydrol.2010.01.020, 2010.
- 430 Fox, G.A., Sabbagh, G.J.: Comment on “Major Factors Influencing the Efficacy of Vegetated Buffers on Sediment Trapping: A Review and Analysis,” by Xingmei Liu, Xuyang Zhang, and Minghua Zhang in the 2008 37:1667–1674. *Journal of Environmental Quality*, 38, 1-3. doi:10.2134/jeq2009.00011e, 2009.
- Gardner WR.: Some steady-state solutions of the unsaturated moisture flow equation with application to evaporation from a water table. *Soil Sci.*, 85(4):228-232, 1958.
- 435 Gillham, R.W.: The capillary fringe and its effect on water-table response, *J. Hydrol.*, Volume 67, Issue 1, Pages 307-324, ISSN 0022-1694, [http://dx.doi.org/10.1016/0022-1694\(84\)90248-8](http://dx.doi.org/10.1016/0022-1694(84)90248-8), 1984.
- Gowdich L, Muñoz-Carpena R.: An improved Green-Ampt infiltration and redistribution method for uneven multistorm series. *Vadose Zone J.*, 8:470-479, doi: 10.2136/vzj2008.0049, 2009.
- Green WH, Ampt GA.: *Studies on Soil Physics*, *J. Agr.Sci.*, 4:1-24, 1911.
- 440 Haan CT, Barfield BJ, Hayes JC.: *Design hydrology and sedimentology for small catchments*. San Diego, Calif.: Academic Press, 1994.
- Holmes JW, Colville JS.: Forest hydrology in a karstic region of Southern Australia. *J. Hydrol.*, 10(1):59-74, 1970.
- Hooghoudt, S.B.: Algemene beschouwing van het probleem van de detailontwatering en de infiltratie door middel van parallel loopende drains, greppels, slooten en kanalen. No. 7 in de serie: Bijdragen tot de kennis van eenige natuurkundige grootheden van den grond. Bodemkundig Instituut te Groningen. Rijksuitgeverij Dienst van de Nederlandse Staatscourant. 's-Gravenhage, Algemeene Landsdrukkerij, 1940.
- 445



- Jury WA, Gardner WR, Gardner WH.: Soil Physics, 5th Edition. John Wiley & Sons, New York, 1991.
- Kao, C., Bouarfa, S., Zimmer, D.: Steady state analysis of unsaturated flow above a shallow water-table aquifer drained by ditches. *J. Hydrol.*, 250, 122–133, doi: 10.1016/S0022-1694(01)00426-7, 2001.
- 450 Lacas, J.-G., Carluier, N., Voltz, M.: Efficiency of a Grass Buffer Strip for Limiting Diuron Losses from an Uphill Vineyard Towards Surface and Subsurface Waters. *Pedosphere*, 22, 580–592, doi: 10.1016/S1002-0160(12)60043-5, 2012.
- Lacas, J.-G., Voltz, M., Gouy, V., Carluier, N., Gril, J.-J.: Using grassed strips to limit pesticide transfer to surface water: a review. *Agron. Sustain. Dev.* 25, 253–266, doi:10.1051/agro:2005001, 2005.
- Lambrechts, T., François, S., Lutts, S., Muñoz-Carpena, R. and Biielders, C. L.: Impact of plant growth and morphology and
455 of sediment concentration on sediment retention efficiency of vegetative filter strips: Flume experiments and VFSSMOD modeling, *J. Hydrol.*, 511, 800–810, doi:10.1016/j.jhydrol.2014.02.030, 2014.
- Liu G, Craig JR, Soulis ED: Applicability of the Green-Ampt infiltration model with shallow boundary conditions. *J. Hydrologic Eng.*, 16:266, doi:10.1061/(ASCE)HE.1943-5584.0000308, 2011.
- Mein RG, Larson CL. Modeling infiltration during a steady rain. *Water Resour. Res.*, 384–394, 1973.
- 460 Miller CT, Williams GA, Kelley CT, Tocci MD.: Robust solution of Richards' equation for non uniform porous media. *Water Resour. Res.*, 34(10):2599–2610, doi:199810.1029/98WR01673, 1998.
- Mualem Y. A new model for predicting the hydraulic conductivity of unsaturated porous media. *Water Resour. Res.*, 12(3):513-522, doi:10.1016/j.cageo.2007.12.002, 1976.
- Muñoz-Carpena, R. & Parsons, J. E.: A design procedure for vegetative filter strips using VFSSMOD-W, *Transactions of the ASAE* 47(6), 1933—1941, doi :10.13031/2013.17806, 2004.
- Muñoz-Carpena, R., Fox, G., Sabbagh, G.: Parameter Importance and Uncertainty in Predicting Runoff Pesticide Reduction with Filter Strips. *Journal of Environmental Quality*, 39, 630–641. doi:10.2134/jeq2009.0300, 2010.
- Muñoz-Carpena, R., Parsons, J.E., Gilliam, J.W.: Modeling hydrology and sediment transport in vegetative filter strips. *J. Hydrol.*, 214, 111–129. doi:10.1016/S0022-1694(98)00272-8, 1999.
- 470 Muñoz-Carpena, R., Ritter, A., Fox G.A., Perez-Ovilla O.: Does mechanistic modeling of filter strip pesticide mass balance and degradation affect environmental exposure assessments? *Chemosphere* 139:410-421. doi:10.1016/j.chemosphere.2015.07.010, 2015.
- Muscutt, A.D., Harris, G.L., Bailey, S.W., Davies, D.B.: Buffer zones to improve water quality: a review of their potential use in UK agriculture. *Agriculture, Ecosystems & Environment*, 45, 59–77, doi:10.1016/0167-8809(93)90059-X, 1993.
- 475 Nash JE, Sutcliffe JV.: River flow forecasting through conceptual models, part I - A discussion of principles. *J. Hydrol.*, 10:282-290, 1970.
- Neuman SP. Wetting front pressure head in the infiltration model of Green and Ampt. *Water Resour. Res.*, 12(3):564-566, doi:197610.1029/WR012i003p00564, 1976.



- 480 Nofziger DL, Wu J.: CHEMFLO-2000: Interactive software for simulating water and chemical movement in unsaturated
soils. U.S.EPA, Cincinnati, Ohio: Rep. EPA/600/R-03/008. National Risk Management Research Laboratory Office of
Research and Development, 2003.
- Ogden FL, Saghafian B. Green and Ampt infiltration with redistribution. *J. Irrigat. Drain. Eng.*, 123, 5, 1997.
- Ogden, F.L., W. Lai, R.C. Steinke, and J. Zhu: Validation of finite water-content vadose zone dynamics method using
column experiment with a moving water table and applied surface flux. *Water Resour. Res.*, 51,
485 doi:10.1002/2014WR016454, 2015.
- Paniconi C, Putti M.: A comparison of Picard and Newton iteration in the numerical solution of multidimensional variably
saturated flow problems. *Water Resour. Res.*, 30(12), 3357, doi:10.1029/94WR02046, 1994.
- Philip JR.: The theory of infiltration: 1. the infiltration equation and its solution. *Soil Sci.*, 83, 5, 345-358, 1957.
- Poletika, N.N., Coody, P.N., Fox, G.A., Sabbagh, G.J., Dolder, S.C., White, J.: Chlorpyrifos and Atrazine Removal from
490 Runoff by Vegetated Filter Strips: Experiments and Predictive Modeling. *Journal of Environmental Quality*, 38, 1042–1052.
doi:10.2134/jeq2008.0404, 2009.
- Press WH, Flannery BP, Teukolsky SA, Vetterling, WT.: *Numerical Recipes in Fortran 77: The Art of Scientific Computing*.
Cambridge University Press, 1992.
- Rawls WJ, Brakensiek DL, Miller N.: Green-Ampt infiltration parameters from soils data. *J. Hydraul. Eng.*, 109(1), 62-70,
495 1983.
- Rawls WJ, Brakensiek DL, Saxton KE.: Estimation of soil water properties. *Trans. ASABE.*, 25(5), 1316-1320, 1982.
- Reichenberger S, Bach M, Skitschak A, Frede H-G.: Mitigation strategies to reduce pesticide inputs into ground- and surface
water and their effectiveness: a review. *Sci. Total Environ.*, 384, 1-35, doi:10.1016/j.scitotenv.2007.04.046, 2007.
- Richards LA.: Capillary conduction of liquids through porous mediums. *Physics.*, 1(5), 318, 1931.
- 500 Ritter, A., Muñoz-Carpena, R.: Performance evaluation of hydrological models: Statistical significance for reducing
subjectivity in goodness-of-fit assessments. *J. Hydrol.* 480, 33–45, doi:10.1016/j.jhydrol.2012.12.004, 2013.
- Ritzema, H.P.: Subsurface flow to drains. Chapter 8 in: H.P.Ritzema (ed.), *Drainage Principles and Applications*, Publ. 16,
pp. 236-304, International Institute for Land Reclamation and Improvement (ILRI), Wageningen, The Netherlands. ISBN 90
70754 3 39, 1994.
- 505 Ross PJ.: Modeling soil water and solute transport—fast, simplified numerical solutions. *Agron. J.*, 95(6), 1352,
doi:10.2134/agronj2003.1352, 2003.
- Sabbagh, G.J., Fox, G.A., Kamanzi, A., Roepke, B., Tang, J.-Z.: Effectiveness of Vegetative Filter Strips in Reducing
Pesticide Loading: Quantifying Pesticide Trapping Efficiency. *J. Environ. Qual.* 38, 762. doi:10.2134/jeq2008.0266, 2009.
- Sabbagh, G.J., Muñoz-Carpena, R. and Fox, G.A. 2013. Distinct influence of filter strips on acute and chronic pesticide
510 aquatic environmental exposure assessments across U.S. EPA scenarios. *Chemosphere* 90(2):195-
202. doi:10.1016/j.chemosphere.2012.06.034



- Salvucci GD, Entekhabi D.: Pondered infiltration into soils bounded by a water table. *Water Resour. Res.*, 31, 2751-2759, doi:10.1029/95WR01954, 1995.
- 515 Seibert J, Rodhe A, Bishop K.: Simulating interactions between saturated and unsaturated storage in a conceptual runoff model. *Hydrol. Process.*, 17(2), 379-390, doi:10.1002/hyp.1130, 2003.
- Simpkins W, Wineland T, Andress R, Johnston D, Caron G, Isenhardt T, Schultz R.: Hydrogeological constraints on riparian buffers for reduction of diffuse pollution: examples from the Bear Creek watershed in Iowa, USA. *Water Science and Tech.* 45, 61-68, 2002.
- Singh VP, Woolhiser DA.: Mathematical Modeling of Watershed Hydrology. *J. Hydrologic Eng.*, 7(4), 270-292, 520 doi:10.1061/(ASCE)1084-0699(2002)7:4(270), 2002.
- Skaggs RW, Huggins LF, Monke EJ, Foster GR.: Experimental evaluation of infiltration equations. *Trans. ASAE.*, 12(6), 822-828, 1969.
- Skaggs RW, Khaleel R.: Infiltration in hydrologic modeling of small watersheds. *ASAE Mon. St. Joseph, MI: Am. Soc. Agr. Engrs.*, 1982.
- 525 Smith RE, Corradini C, Melone F.: Modeling infiltration for multistorm runoff events. *Water Resour. Res.*, 29(1), 133-144, doi:10.1029/92WR02093, 1993.
- Smith RE, Smettem KRJ, Broadbridge P.: Infiltration theory for hydrologic applications. American Geophysical Union, Washington, DC: *Water Res. M.*, 15, 2002.
- Srivastava R, Yeh T-CJ.: Analytical solutions for one-dimensional, transient infiltration toward the water table in 530 homogeneous and layered soils. *Water Resour. Res.*, 27(5), 753-762, doi:10.1029/90WR02772, 1991.
- Talbot, C. A., and F. L. Ogden: A method for computing infiltration and redistribution in a discretized moisture content domain, *Water Resour. Res.*, 44, W08453, doi:10.1029/2008WR006815, 2008.
- Vachaud G, Gaudet JP, and Kuraz V.: Air and water flow during ponded infiltration in a vertical bounded column of soil. *J. Hydrol.*, 22, 89-108, doi: 10.1016/0022-1694(74)90098-5, 1974.
- 535 Vachaud G, Thony JL.: Hysteresis during infiltration and redistribution in a soil column at different initial water contents. *Water Resour. Res.*, 7, 111-127, doi:10.1029/WR007i001p00111, 1971.
- van Genuchten MT.: A closed-form equation for predicting the hydraulic conductivity of unsaturated soils. *Soil Sci. Soc. Am. J.*, 44, 892-898, 1980.
- van Hoorn J.W., van Der Molen W.H.: Drainage of sloping lands, *Design and management of drainage system.*, 329-339, 540 1973.
- van Schilfgaarde, J.: Approximate solutions to drainage flow problems. In: J.N.Luthin (Ed.), *Drainage of agricultural lands*, p.79-112. *Agron. Monogr. 7.* ASA, Madison, WI, USA, 1957.
- Vertessy R.A., Hatton T.J., O'Shaughnessy P.J., Jayasuriya M.D.A.: Predicting water yield from a mountain ash forest catchment using a terrain analysis based catchment model, *J. Hydrol.*, 665-700, doi:10.1016/0022-1694(93)90131-R, 1993.



- 545 Vogel T, van Genuchten MT, Cislérova M.: Effect of the shape of the soil hydraulic functions near saturation on variably-saturated flow predictions. *Adv. Water Resour.*, 24(2), 133-144, doi:10.1016/S0309-1708(00)00037-3, 2001.
- Wu, L., Muñoz-Carpena, R., Gao, B., Yang, W. and Pachepsky, Y. A.: Colloid Filtration in Surface Dense Vegetation: Experimental Results and Theoretical Predictions, *Environ. Sci. Technol.*, 48(7), 3883–3890, doi:10.1021/es404603g, 2014.
- 550 Yu, C., Muñoz-Carpena, R., Gao, B. and Perez-Ovilla, O.: Effects of ionic strength, particle size, flow rate, and vegetation type on colloid transport through a dense vegetation saturated soil system: Experiments and modeling, *J. Hydrol.*, 499, 316–323, doi:10.1016/j.jhydrol.2013.07.004, 2013.



552 Table 1. Parameters used in numerical and experimental testing of SWINGO. Nash and Sutcliffe coefficient of efficiency (C_{eff}) and root mean error (RMSE) represent
 553 SWINGO infiltration goodness-of-fit with Richards' finite differences solution (CHEMFLO-2000) and experimental data from Vachaud et al., (1974).

Numerical testing [†]										
Soil	L (m)	θ_r	θ_s	K_s ($m \cdot s^{-1}$)	h_b (m)	λ	η	$C_{eff}^{††††††††}$	RMSE ^{††††} f ($\times 10^{-6} m \cdot s^{-1}$)	
Silty Loam	1.5	0	0.35	3.40×10^{-6}	0.450	1.20	4.67	0.994[0.969-0.999] ^{***}	0.309[0.119-0.541]	
Clay	1.5	0	0.45	3.40×10^{-7}	0.900	0.44	7.54	0.999[0.998-1.000] ^{***}	0.015[0.003-0.028]	
Sandy Loam	1.5	0	0.25	3.40×10^{-5}	0.250	3.30	3.61	0.985[0.882-0.998] ^{***}	1.326[0.578-2.414]	
Vachaud and Thony (1971)	1.01	0	0.35	1.75×10^{-5}	0.181	0.73	4.63	0.927[0.821-0.977] ^{***}	1.488[0.893-2.240]	

Experimental testing ^{††††}										
Soil	L (m)	θ_r	θ_r	K_s ($m \cdot s^{-1}$)	α_{vG} (m^{-1})	n	m	α_{Grd} (m^{-1})	n_{Grd}	RMSE ^{††††} f ($\times 10^{-6} m \cdot s^{-1}$)
Vachaud et al., (1974)	0.925	0.107	0.34	2.64×10^{-5}	1.143	2.363	0.652	-	0.913[0.742-0.951] ^{**}	6.204[4.726-7.920]
vG/vG	0.925	0.107	0.34	2.64×10^{-5}	1.143	2.363	0.652	0.136	2.151	0.942[0.828-0.971] ^{***}
vG/Grd	0.925	0.107	0.34	2.64×10^{-5}	1.143	2.363	0.652	0.136	2.151	0.942[0.828-0.971] ^{***}

554 [†] h_b , λ , η are the Brooks and Corey parameters; ^{††} α_{vG} , n , and m are van Genuchten parameters, and α_{Grd} and n_{Grd} are the Gardner parameters (see Appendix for
 555 details); ^{†††} median value [95% confidence interval in brackets]; ^{††††} models were statistically acceptable at a significance level of 0.01 (^{***}) or 0.05 (^{**}) (Ritter and
 556 Muñoz-Carpena, 2013)



557 **Table 2. Infiltration and excess runoff calculations for an illustrative unsteady rainfall event on a clay soil with no initial**
 558 **ponding at equilibrium with a shallow water table at 150 cm depth ($s_{max}=0$). The + sign in the first column represents any**
 559 **time right after the time step.**

<i>Time, t</i>	<i>t_p</i>	<i>t₀</i>	<i>t_w</i>	<i>i</i>	<i>P</i>	<i>f</i>	<i>F</i>	<i>RO</i>	<i>z_F</i>
(s)	(s)	(s)	(s)	(m/s)	(m)	(m/s)	(m)	(m)	(m)
0	4657.2	2319.0	16100	2.78×10^{-6}	0	2.78×10^{-6}	0.0000	0	0
4657.2	4657.2	2319.0	16100	2.78×10^{-6}	0.0129	2.78×10^{-6}	0.0129	0	0.017
7500				2.78×10^{-6}	0.0208	1.83×10^{-6}	0.0192	0.0016	0.253
10000				2.78×10^{-6}	0.0278	1.46×10^{-6}	0.0233	0.0045	0.327
10000 ⁺				7.00×10^{-7}	0.0278	7.00×10^{-7}	0.0233	0.0045	0.327
15000				7.00×10^{-7}	0.0313	7.00×10^{-7}	0.0268	0.0045	0.408
15000 ⁺	15000	13763.7	18500	2.78×10^{-6}	0.0313	1.21×10^{-6}	0.0268	0.0045	0.408
16500	15000	13763.7	18500	2.78×10^{-6}	0.0354	1.08×10^{-6}	0.0285	0.0069	0.461
18000				2.78×10^{-6}	0.0396	9.49×10^{-7}	0.0300	0.0096	0.535
18000 ⁺				7.00×10^{-7}	0.0396	7.00×10^{-7}	0.0300	0.0096	0.535
18500				7.00×10^{-7}	0.0399	7.00×10^{-7}	0.0304	0.0096	0.569
18500 ⁺				7.00×10^{-7}	0.0399	3.40×10^{-7}	0.0304	0.0096	0.600
25000				7.00×10^{-7}	0.0445	3.40×10^{-7}	0.0326	0.0119	0.600
25000 ⁺				0	0.0445	0	0.0326	0.0119	0.600

560

561 **FIGURE CAPTIONS**

562 **Figure 1:** Conceptual depiction of infiltration and soil water redistribution for soils with shallow water table for: a) time
563 before wetting front reaches the water table; and b) time after the wetting front reaches the water table ($t \geq t_w$), where
564 surface infiltration flow (Q_f) is limited by lateral Boussinesq subsurface flow (Q_L). See explanation of symbols in the text.

565 **Figure 2:** Conceptual curves of (a) infiltration rate, f ; (b) cumulative infiltration, F ; and (c) soil water redistribution, θ ,
566 under shallow water table, for soil without initial ponding, and constant rainfall rate (i) conditions. The singular times for
567 ponding (t_p), shifting (t_d) and to reach column saturation (t_w), and final infiltration rate (f_w) after the wetting front reaches
568 the water table ($t \geq t_w$) are represented.

569 **Figure 3:** Comparison of normalized infiltration rates (f/K_s) obtained with the simplified model (lines) against Richards
570 equation numerical solution (symbols) for soils without initial ponding in Table 1 with vertical drainage (Vachaud) bottom
571 boundary (f_w) conditions.

572 **Figure 4:** (a) Comparison of cumulative infiltration (F) obtained with the simplified model (lines) against Richards
573 equation numerical solution (symbols) for soils without initial ponding in Table 1 with vertical drainage (Vachaud) bottom
574 boundary (f_w) condition; (b) Wetting front depth (z_f) movement.

575 **Figure 5:** Comparison of soil water (θ) redistribution between Richards equation numerical solution (solid lines) and the
576 simplified model (dashed lines) during infiltration without initial ponding and with vertical drainage (Vachaud) bottom
577 boundary condition (f_w) for soils in Table 1.

578 **Figure 6:** Comparison of the simplified and RE results against Vachaud et al., (1974) experimental data set (figure body),
579 and fitting of soil water characteristics to different equations (inset). vG and Grd represent respectively the van
580 Genuchten and Gardner's soil characteristic curves used to parametrize the simplified and RE models (see Table 1 for
581 details).

582 **Figure 7:** Calculations for an unsteady rainfall event on clay soil in initial equilibrium with a shallow water table at 150 cm
583 depth, non-ponded conditions and vertical drainage (Vachaud) bottom boundary condition (f_w): a) infiltration and rainfall
584 rates; b) cumulative rainfall (P), infiltration (F), excess runoff (RO) and wetting front depth (z_f) during the event.

585 **Figure 8:** Effect of water table depth (L) on cumulative infiltration (F , represented by isolines) for distinct soils under
586 initial ponding and different durations of infiltration events (D) for four types of soils and two end drainage bottom
587 boundary conditions (f_w): (a-d) vertical; (e-h) lateral.

588 **Figure 9:** Cumulative infiltration (F , represented by isolines) as a function of water table depth (L) under non-ponded
589 initial conditions after a 6 hour rainfall event of intensity i for four types of soils and two end drainage bottom boundary
590 conditions (f_w): (a-d) vertical (e-h) and lateral.

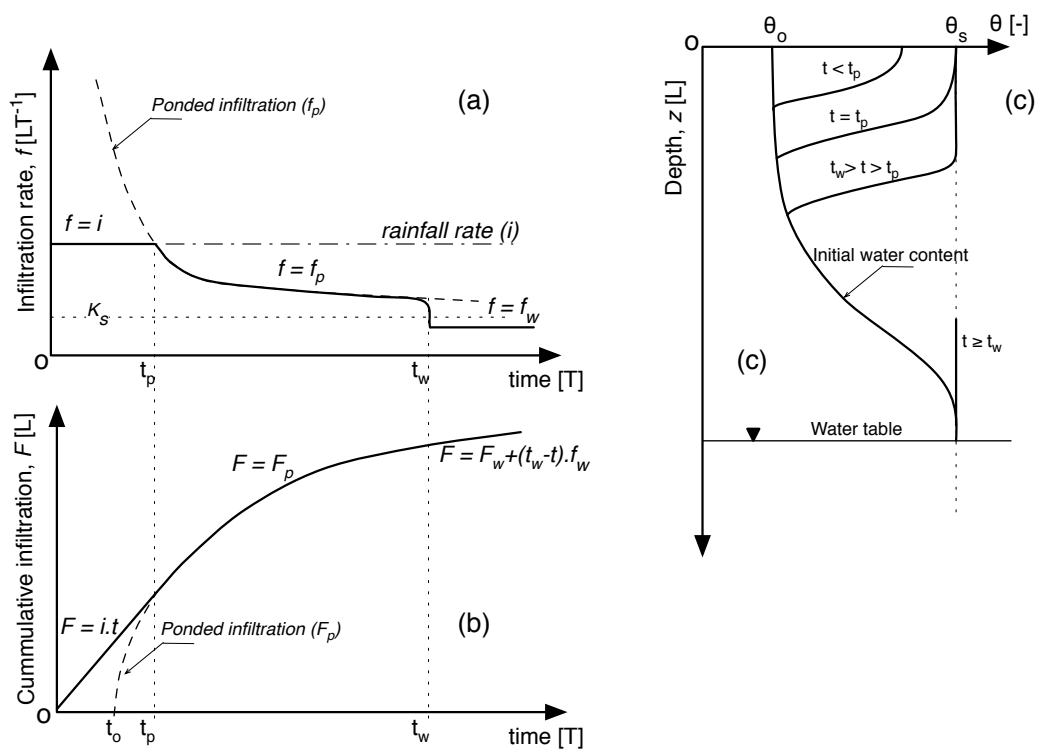


FIG. 2

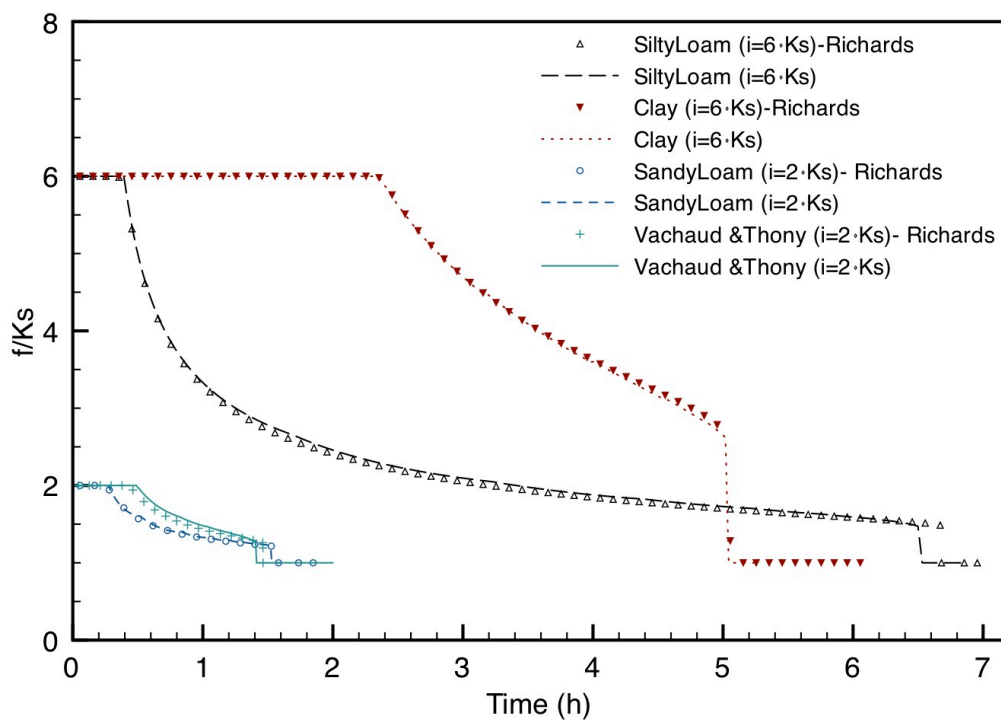


FIG. 3

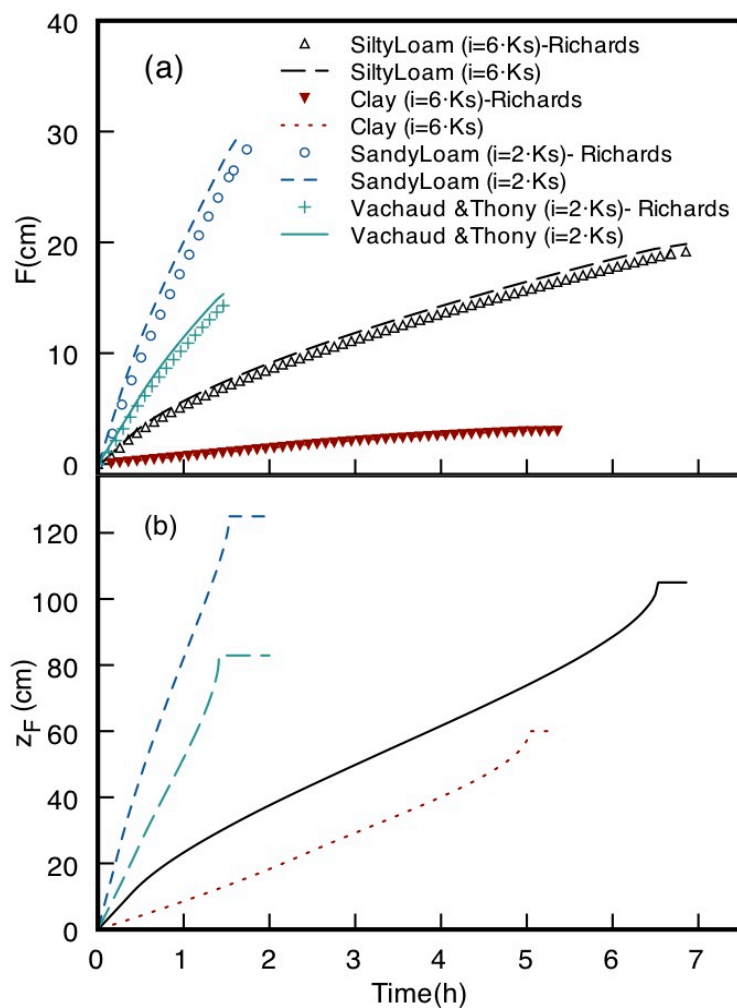


FIG. 4

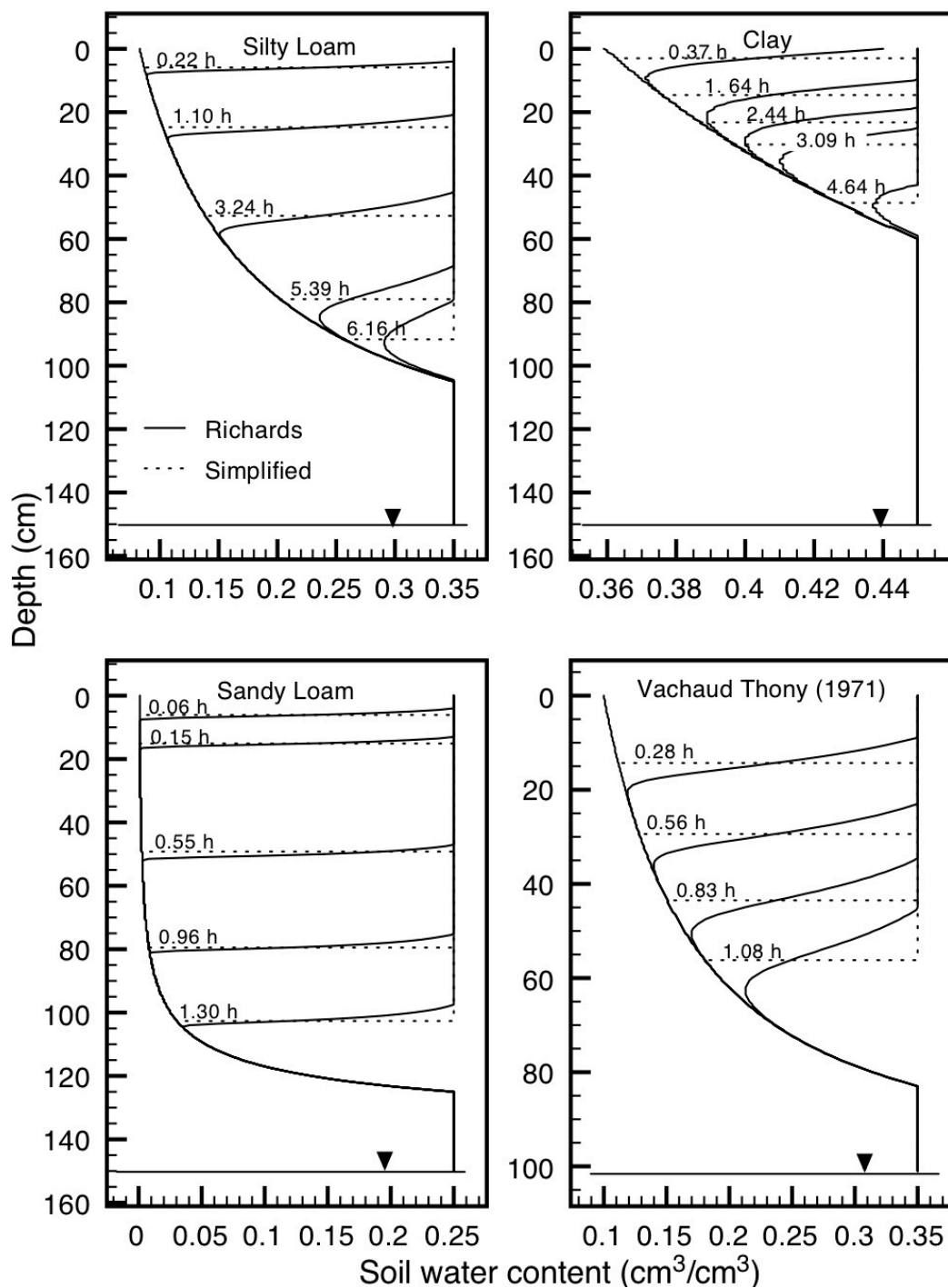


FIG. 5

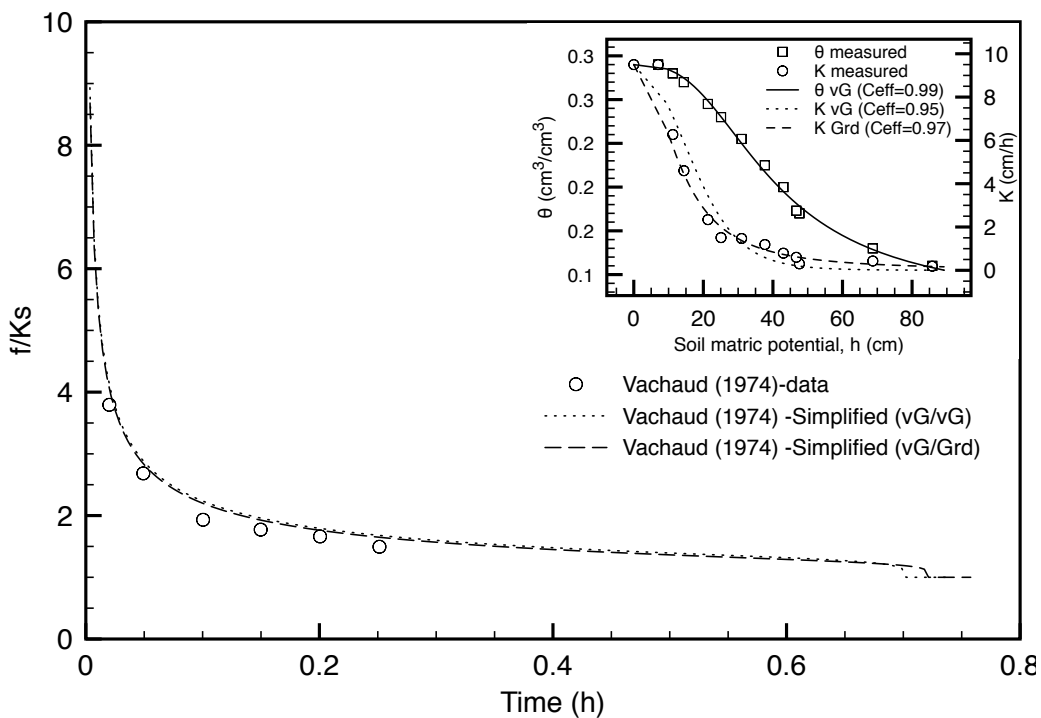


FIG. 6

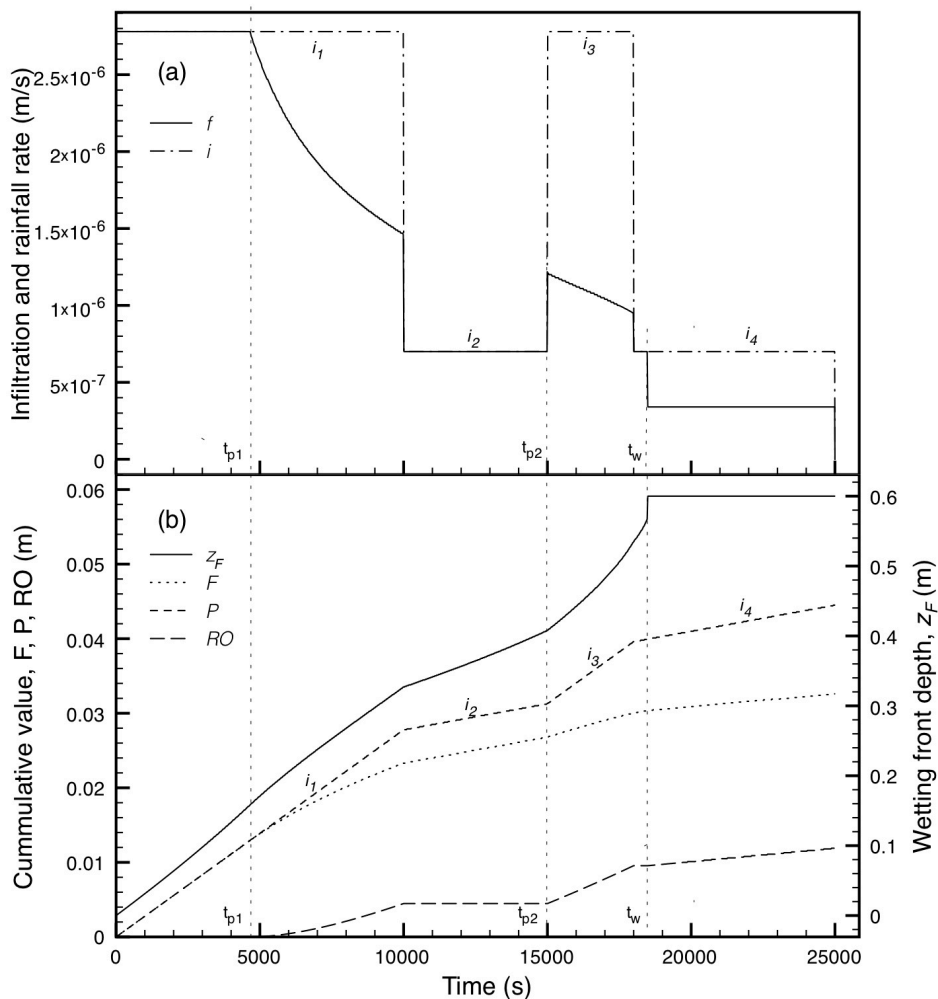


FIG. 7

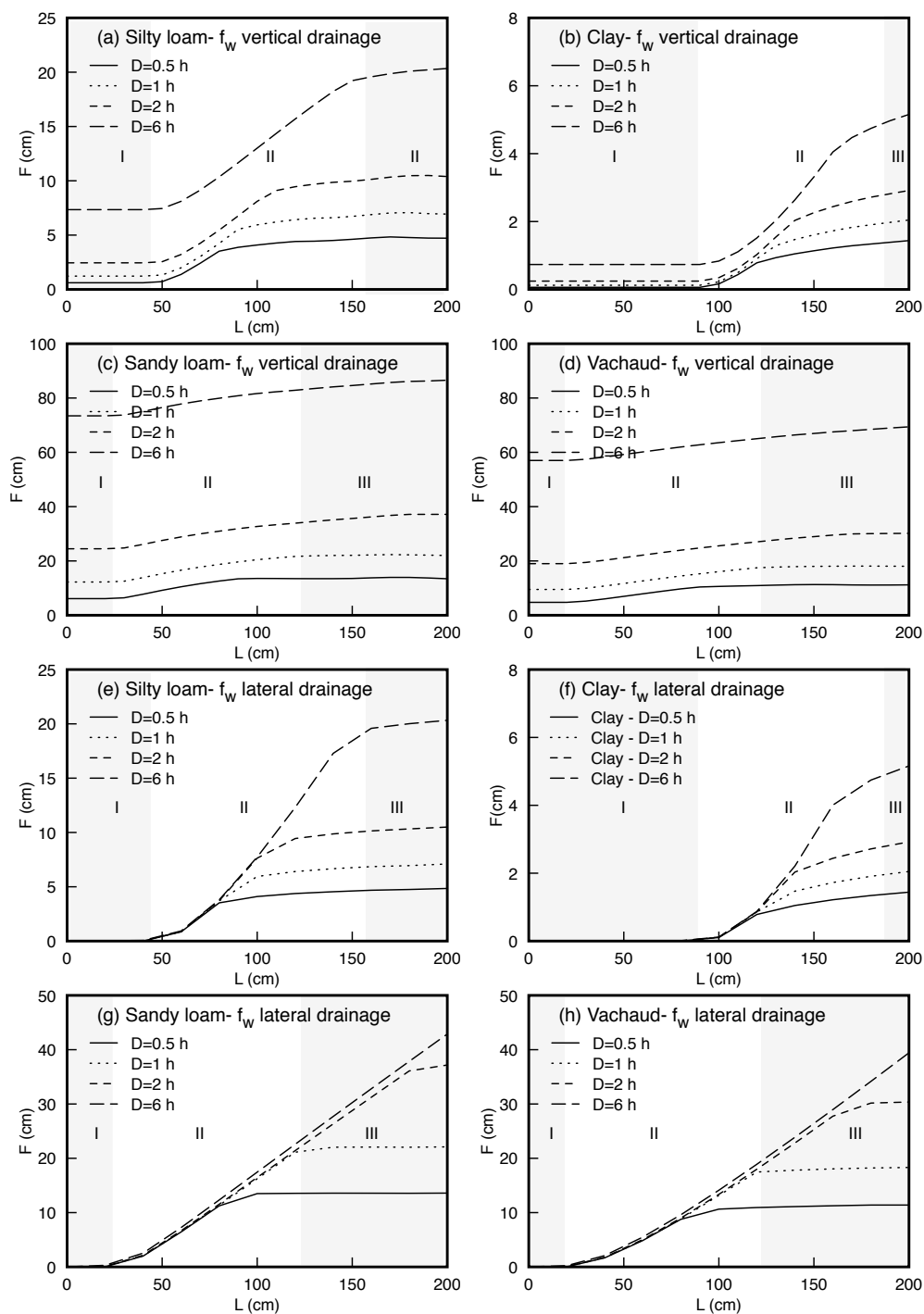


FIG. 8

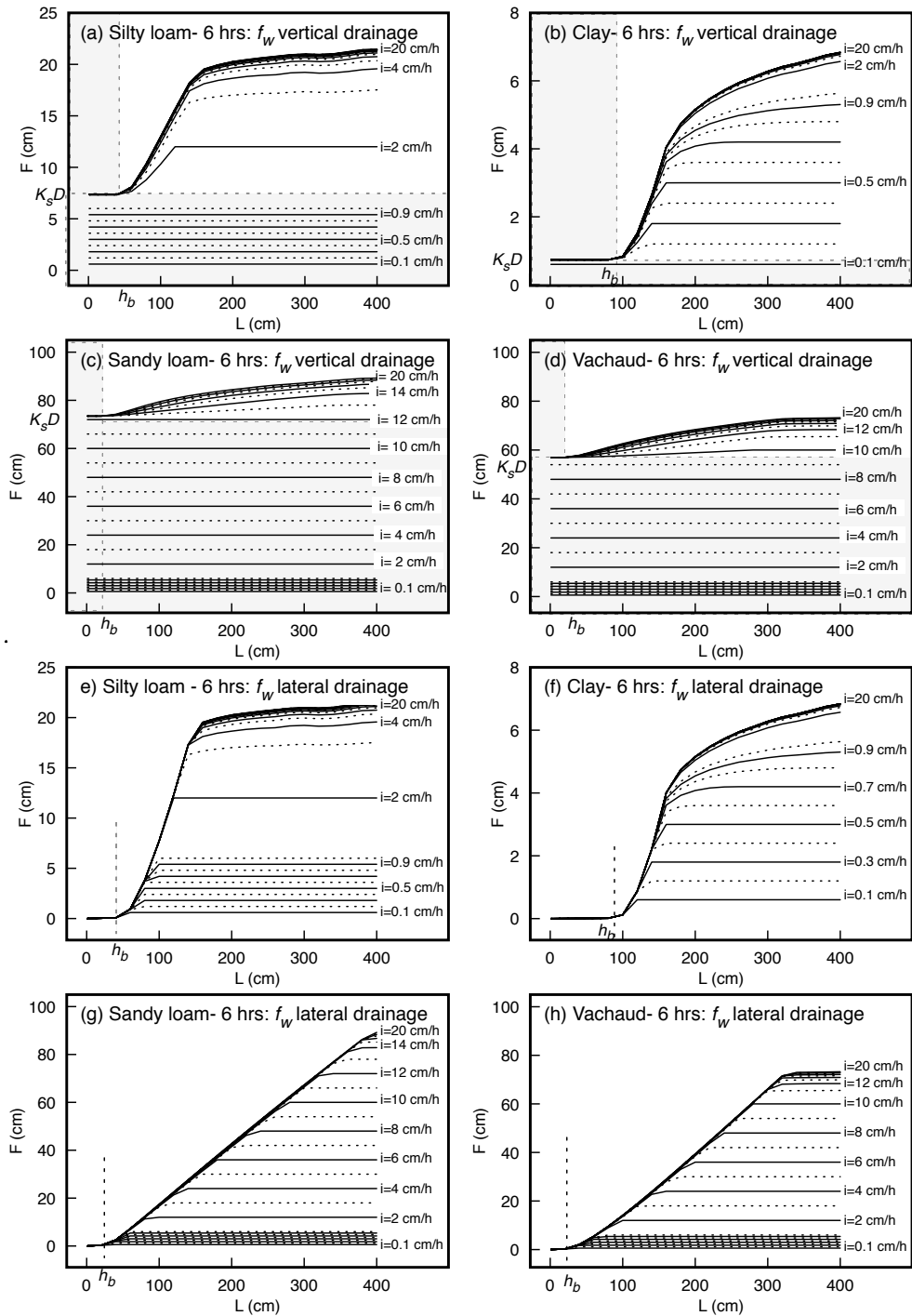


FIG. 9